buildings

MDPI

Article

Experimental Study of an Industrial Tower-Type Supporting Frame with Facades Subjected to the Stationary Wind Effect

Lyudmila Frishter [1,*] and Maxim Lukin [2]

[1] Department of Higher Mathematics, National Research Moscow State Civil Engineering University, 26, Yaroslavskoye Shosse, 129337 Moscow, Russia
[2] Building and Construction Department No. 1 (SMU No. 1 LLC), 17, Nauchny Proyezd, 117246 Moscow, Russia
* Correspondence: frishterly@mgsu.ru

Abstract: Aerodynamic studies of canceled structures are important for design of buildings, analysis of air flows inside buildings, evaluation of buildings' effects on air flow patterns of the adjoining area, and optimal choice of enclosing structures. The analysis of wind effects during the design of canceled structures is governed by codes and standards of general purpose. These statutory documents do not regulate the mounting procedure of wind protection screens, nor do they contain the analysis of wind effects on structures with different angles of attack of an incident wind flow. The codes prescribe aeroelastic model testing in special civil engineering wind tunnels during the design of such structures. The purpose of this research project is to analyze wind effects on the force and torque specification of a canceled structure at different wind effect angles accounting for the mounting sequence of wind protection screens. The subject of the article is an experimental aeroelastic study of wind effects on a canceled structure accounting for sequential mounting of wind protection screens on the structure's facade. The obtained data will allow for the analysis of effects of the wind flow angle on internal forces of the structure, given that a change in its permeability is taken into account. At the initial design stage, experimental modeling of wind effects in a wind tunnel is thereby considered a structure model validation step. The relevance of the paper lies in the need to identify optimum operating conditions of canceled structures, subjected to a wind effect, to ensure safe and comfortable work of people and reliable operation of process equipment installed inside the facility.

Keywords: canceled structure; wind effect; wind protection screens; experimental aerodynamic studies; force and torque specifications

check for updates

Citation: Frishter, L.; Lukin, M. Experimental Study of an Industrial Tower-Type Supporting Frame with Facades Subjected to the Stationary Wind Effect. *Buildings* **2023**, *13*, 866. https://doi.org/10.3390/buildings13040866

Academic Editor: Theodore Stathopoulos

Received: 2 February 2023
Revised: 20 March 2023
Accepted: 23 March 2023
Published: 26 March 2023

Copyright: © 2023 by the authors. Licensee MDPI, Basel, Switzerland. This article is an open access article distributed under the terms and conditions of the Creative Commons Attribution (CC BY) license (https://creativecommons.org/licenses/by/4.0/).

1. Introduction

Canceled structures are used in the course of construction of buildings and structures, as storage for materials and a place for engineering equipment. They are cheap and easy to install. The design of canceled structures includes analysis of the stress–strain state in case of wind effects [1–12].

The analysis of wind effects during the design of civil structures is subject to the following applicable codes: SP 20.13330.2016 "SNiP 2.01.07-85* Loads and Effects"; SP 296.1325800.2017 "Buildings and facilities. Special effects"; GOST R 56728–2015 "Buildings and facilities. Method of determining wind effects on enclosing structures"; Civil Codes of Belarus. TKP EN 1991-1-4-2009 (02250 and national supplement. Eurocode 1. Effects onto structures. Part 1-4. General effects. Wind effects), with finalizing indications and explanations [13–18], journal articles, Journal of Wind Engineering & Industrial Aerodynamics, Engineering Structures, Physics of Fluids, etc.

The wind load on a building is determined by its shape, spatial position, and enclosure permeability. SP 20.13330.2016 SNiP 2.01.07-85* prescribes considering the following factors in the process of analyzing wind loads on buildings and structures:

(1) Prevailing wind load type.
(2) Peak wind loads on structural enclosure elements and mounting elements thereof.
(3) Resonant vortex excitations.
(4) Aerodynamically unstable oscillations such as galloping, divergence, and flatter.

As for the open-type canceled structure, wind effects create uncomfortable conditions for the work of people and equipment operation inside. Installation of wind screens on the facade of a structure changes its permeability and internal forces [1–4,19].

Pursuant to SNiP 2.01.07-85* on "Prevailing wind load types", the mean component of the wind load is addressed, while the fluctuating component of the wind load is disregarded.

During the erection of a building, when the structure is screened against the wind, or in the absence of enclosure walls, changes in wind pressure on the structure, in the enclosure permeability, and in internal forces are possible which must also be taken into consideration in the structure design.

Mounting sequences of screens are considered: first, on one side, then, on two sides, three sides, and the whole vertical enclosure. This allows analyzing the influence of the screen mounting sequence on forces induced in the structure under a wind effect.

The SNiP 2.01.07-85* code does not specify the sequence of the wind protection screen installation, not allowing for the analysis of the wind direction change. During the design of such structures, the codes prescribe aeroelastic model testing in special civil engineering wind tunnels.

Each special wind tunnel is original; it has its own design features and aerodynamic characteristics.

The experimental study of the wind flow effect on a structure in the wind tunnel needs an experimental methodology in compliance with the problem statement in mechanics. The problem of aeroelasticity is considered as a study of internal forces of a canceled structure under the steady action of a wind flow.

Changes in the direction of the effect of a wind flow on the front surface of the structure, including the angle of attack and the sequence of installation of wind screens onto the structure, are taken into account.

Objectives of the work:

(1) development of the experiment procedure; experimental studies of the wind effect on a canceled structure rectangular in plan;
(2) consideration of the effect of the wind flow angle on a change in the internal forces of a building;
(3) consideration of the effect of the sequence of installation of wind screens on a change in the internal forces of a building;
(4) analysis of internal forces of a canceled structure in case of a change in the direction of a wind flow focused on the structure and sequence of installation of screens on the building facade.

A physical modeling of the wind air flow effect was performed on a canceled structure in a specialized wind tunnel of the Academic, Scientific and Industrial Laboratory of Aerodynamics and Aeroacoustics (ASIL ADAC MGSU). At the university formerly known as MISI and now known as MGSU, in the 1960s, methods of experimental solving of aerodynamic problems in architecture and civil engineering [1,3,4,19] were developed, including an algorithm developed for the wind mode analysis in urban development [1,4,19]. The methodology of the experiment was determined by the design of the wind tunnel.

The wind tunnel, used for architectural and civil engineering purposes and currently operated by MGSU (Figure 1), has original design features.



Figure 1. The wind tunnel for architectural and civil engineering purposes at MGSU.

Methods of simulating wind air flows, surrounding the aeroelastic model of a structure or a facility in the wind tunnel of MGSU, are described in papers [20–24]. Studies of gas flows, surrounding fixed aeroelastic models of structures, are governed by the structure design objectives and the aerodynamics of industrial buildings [23–27].

Analysis of the wind load on a structure includes physical, mathematical, and numerical modeling [8,9,16,28,29] of "wind aerodynamics problems based on numerical solutions to 3D equations of liquid and gas motion with adequate turbulence models implemented in modern verified licensed software environments of computational fluid dynamics" [16].

The results of physical modeling in the wind tunnel are the data used to solve the general problem of complex physical, mathematical, and numerical modeling of the stress–strain state of canceled structures. The data obtained in the experiment can be applied as the data for validation of the results of a more detailed modeling of loads on a structure [30].

It is an objective of the study to analyze the wind effects on the force and torque specification of a canceled structure at different wind effect angles with account taken of the mounting sequence of wind protection screens.

The relevance of the paper lies in the need to determine the optimum conditions of operation of canceled structures under wind effects to ensure the safe and comfortable work of people and reliable operation of process equipment installed inside the facility.

The practical significance of the work is determined by the recommendations for the optimal operation of a structure and comfortable work of people in case of wind effects, depending on the location of the structure and installation of protective screens on it.

2. Materials and Methods. Experimental Aeroelastic Studies of a Canceled Structure

2.1. Object of Study

The canceled structure is rectangular; its length is L = ξ, its height is H = 3/4ξ, and its width is 5/8ξ, where ξ is the characteristic dimension. Figure 2 is a drawing of the structure. Mesh spacing is the same lengthwise: L0 = L/4 = ξ/4, heightwise: H0 = H/5 = ξ/8, widthwise: b0 = b/5 = ξ/8.

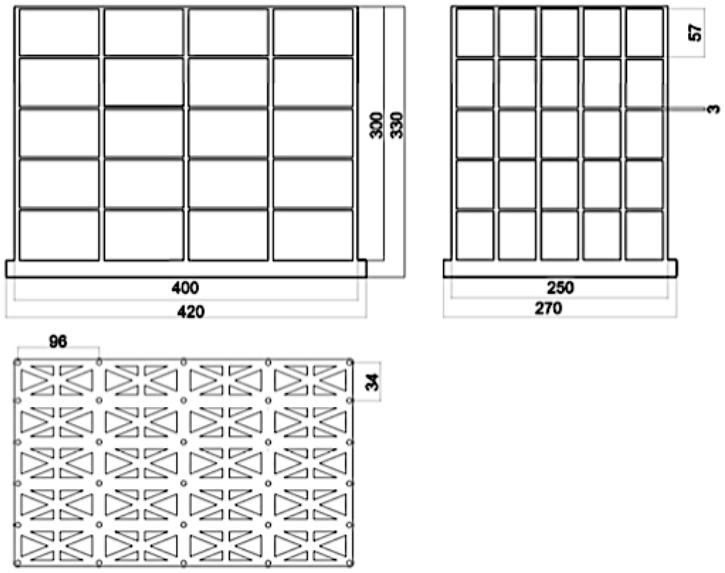


Figure 2. Canceled structure.

2.2. Problem Statement

The wind effect on the canceled structure is studied experimentally in a wind tunnel. The aeroelastic model is erected in the wind tunnel section and subjected to a flat steady air flow. Due to the steady nature of the flow, all components containing partial derivatives of time are equal to zero in the motion and continuity equation. The flat steady flow can be considered as a test model of gas dynamics. No pressure change on the structure surface is measured.

Flat steady flows without recognition of volume forces suit the following resolving system of equations [1,2,5,19]:

Continuity equation:

$$\frac{\partial(\rho V_x)}{\partial x} + \frac{\partial(\rho V_y)}{\partial y} = 0,$$

Momentum conservation equation:

$$\frac{1}{\rho}\frac{\partial p}{\partial x} + \frac{\partial}{\partial x}\left(\frac{V^2}{2}\right) = V_y\left(\frac{\partial V_y}{\partial x} - \frac{\partial V_x}{\partial y}\right), \frac{1}{\rho}\frac{\partial p}{\partial y} + \frac{\partial}{\partial y}\left(\frac{V^2}{2}\right) = -V_x\left(\frac{\partial V_y}{\partial x} - \frac{\partial V_x}{\partial y}\right),$$

Energy conservation equation:

$$\frac{d}{dt}\left(\frac{p}{\rho^\gamma}\right) \equiv V_x\frac{\partial}{\partial x}\left(\frac{p}{\rho^\gamma}\right) + V_y\frac{\partial}{\partial y}\left(\frac{p}{\rho^\gamma}\right) = 0,$$

where V is the flow velocity, $V = \sqrt{V_x^2 + V_y^2}$,V_x, V_y are the flow velocity components along OX, OY axes, respectively, p is pressure, ρ is gas (air) flow density, γ is the isentropic exponent (γ = cp/cv), cp, cv are specific thermal capacities of the gas mix.

For vortex-free motion, we obtain:

$$\frac{\partial V_y}{\partial x} - \frac{\partial V_x}{\partial y} = 0.$$

For a vortex-free steady one-dimensional flow in the absence of mass forces, the resulting momentum equations are converted to the Bernoulli equation:

$$\rho V dv = dp \text{ or } p + \frac{\rho V^2}{2} = const. \quad (1)$$

Equation (1) is applied to small Mach numbers M < 0.4. When the cross section of the jet is changed, the air is practically incompressible; its density, temperature, and internal energy do not change. At critical points of the model surface, the flow "sticks" to the boundary of the structure, and its velocity along the boundary of the area is zero.

The quasi-static problem of elasticity is solved for the case of constant flow influence; internal forces are determined taking into account changes in the flow direction on the structure and permeability of the structure in the event of successive installation of facade screens.

2.3. Theoretical Provisions of Experimental Problem Solving

The experimental studies of the air flow effect on the structure are conducted within the flow section, where a flat steady flow can be reduced to a single-axis vortex-free steady flow. The steady wind flow, affecting the structure and the angle of incidence of the wind airflow, are constant along the external surface of the structure.

During the testing of an aeroelastic model in the wind tunnel, the assurance of similarity between the aerodynamic flow characteristics and the full-scale situation deserves thorough analysis. When dimensions of a full-scale structure are reduced by hundreds of times, the similarity of the Reynolds number requires respective multiplication of the air flow velocity in the tunnel. Thereby, the air flow velocity in the tunnel would exceed 50–100 m/s, which is why, during scaled model testing in the wind tunnel, a full-scale Reynolds number $Re \approx 2 \times 10^7$ match is impossible [20–22].

For similar class structures (high-drag bodies), there is a so-called "self-similarity range by Reynolds number *Re*", where an increase in the number leads to the loss of dependency of the flow behavior of the body on this parameter [5,20–22]. Detailed studies of the aerodynamic characteristics of a flow for this wind tunnel, operating at MSCU, are addressed in papers [5,11,20–22] and used in the work.

To determine the self-similarity range using the Reynolds number of the tested aeroelastic model, auxiliary tests are conducted at the consequential increase in the air flow velocity $V\infty$ in the tunnel from 5 to 30 m/s.

The obtained dependencies allow concluding that for the aeroelastic model there is self-similarity by the Reynolds number $Re < 1 \times 10^5$ at air flow velocities $V\infty \geq 7$ m/s [5,11,20–22].

The experiment covers the case where a single-axis wind flow interacts with an obstacle—the canceled structure. The magnitudes of the aerodynamic factors for the longitudinal, vertical, and transversal forces, respectively, are determined in accordance with SP 20.13330.2016 "SNiP 2.01.07-85*", TKP EN 1991-1-4-2009:

$$C_x = \frac{F_x}{q_\infty S}, C_y = \frac{F_y}{q_\infty S}, C_z = \frac{F_z}{q_\infty S},$$

where $q_\infty == (\rho_\infty V_\infty^2)/2$ is velocity head, characteristic area S, ρ_∞, V_∞ are density and velocity of undisturbed flow. Relative dynamic factors are not considered.

The interaction of the flow with the facility is complicated by open inner spaces of the canceled structure changing due to the mounting of screens on the building facade.

2.4. Aeroelastic Model Design and Production

For experimental studies, an aeroelastic model of an industrial tower-type supporting frame is developed and made. The aeroelastic model has a layout size of 250 mm × 400 mm; the height is 300 mm. Permeable floors are uniformly distributed across the structure's height with 60 mm vertical pitch, starting from the ground level, up to the top elevation mark of the structure. Given the dimensions of the testing section of the wind tunnel, the maximum model scale of 1:100 is selected.

The aeroelastic model is made of steel M6 pins imitating vertical columns. The floors and their elements (levels 1–5) are made of a solid acrylic glass work piece. Steel pins are screwed into the plywood plate used as the aeroelastic model base. After that, acrylic glass plates are threaded on the pins with prepared holes. Acrylic glass plates are fastened with

steel nuts; the nuts are locked on the top and bottom with glue to prevent unscrewing and to retain the aeroelastic model floor level.

After installation of each aeroelastic model floor level, horizontality is checked with a digital inclinometer in the middle of the aeroelastic model.

After the final assembly of all necessary parts, the final dimensional check of the finished aeroelastic model of an industrial tower-type supporting frame is performed (Figure 3).



Figure 3. Aeroelastic model of an industrial tower-type supporting frame.

In the aeroelastic model production stage, a 6-channel force and torque sensor is installed to measure resulting aerodynamic forces and torques. The sensor is fastened to a rigid metal plate in the aeroelastic model base. The assembled aeroelastic model is installed on an automated turntable in the test section of the wind tunnel.

2.5. Experimental Fixture and Measurement Devices

2.5.1. Characteristics of the Wind Tunnel

Wind tunnel laboratory at MGSU (Figure 1)(hereinafter—MGSU wind tunnel) has a closed circulation loop and a modular fan block consisting of nine units. Characteristics of MGSU wind tunnel:

- the length of the axis of the closed loop of the MGSU wind tunnel is 96 m;
- the length of the working zone of the MGSU wind tunnel of 18.9 m and it allows correcting the flow velocity profile, simulating the surface layer of the atmosphere under different conditions;
- the direction of the flow path of MGSU wind tunnel is horizontal;
- the diameter of the turntable is 3 m;
- the velocity range in the working zone is 0 to 32 m/s;
- the power of the fan unit is 333 kW;
- the irregularity of the velocity diagram of the incoming flow does not exceed 2.5% at a flow velocity $V\infty$ = 12 m/s.

In the experiment, measurements are taken at a flow velocity $V\infty$ = 12 m/s. Dimensionless aerodynamic coefficients of the scale model, obtained in the aerodynamic experiment, are similar to the corresponding values in natural conditions [1–5,18,25] and are not considered in this work.

2.5.2. Measuring Equipment

To measure forces and torques, a Schunk FTD load-cell type scale (SCHUNK GmbH & Co. KG, Production facility, Bahnhof str. 106–134, D-74348 Lauffen/Neckar, Germany) is used. It has small six-channel force and torque measurement transducers (Figure 4). Sensors are installed in the base (Figure 5).

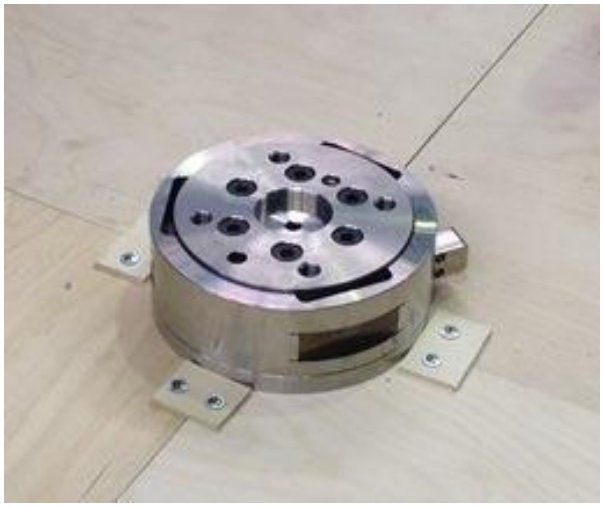


Figure 4. Schunk FTD strain gauge.

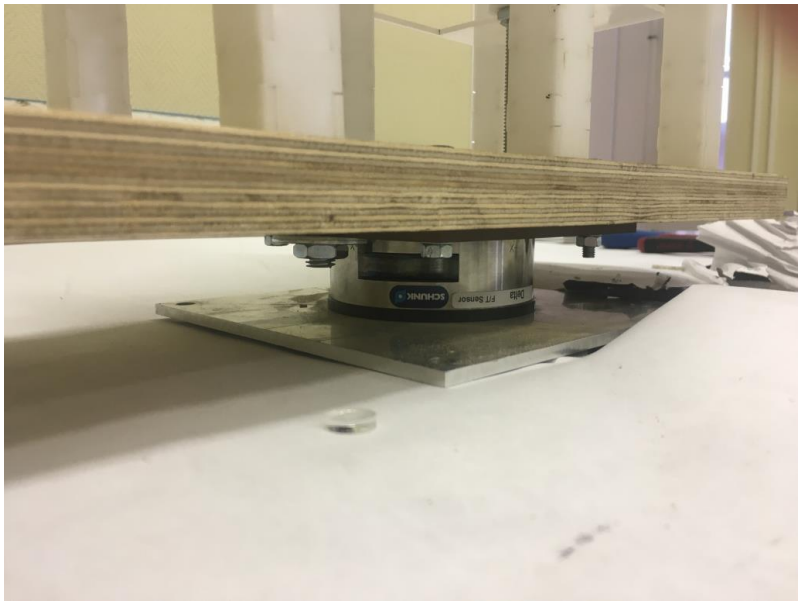


Figure 5. A 6-piece force–moment sensor at the base of the model.

Force measurement range Fx, Fy: ±1 kN; Fz: ±2.5 kN; Mx, My: ±120 Nm; Mz: 120 Nm. Force measurement accuracy Fx, Fy, Fz: ±1/16 N. Torque measurement accuracy: Mx, My: ±1/160 Nm; Mz: ±1/320 Nm.

The load-cell scale (Figure 4) is of solid design ensuring transformation of the measured forces and torques to analog output signals of the load cell. The obtained data are processed by the standard freeware computing torque and force values. The calibration table is provided by the load-cell scale manufacturer.

2.6. Experimental Aeroelastic Study of the Wind Load on the Model

The aeroelastic model of an industrial tower-type supporting frame is installed in the test section of the wind tunnel on a rotary platform to study the effects of the wind direction change (wind flow angles of incidence) on the structure (Figure 6).

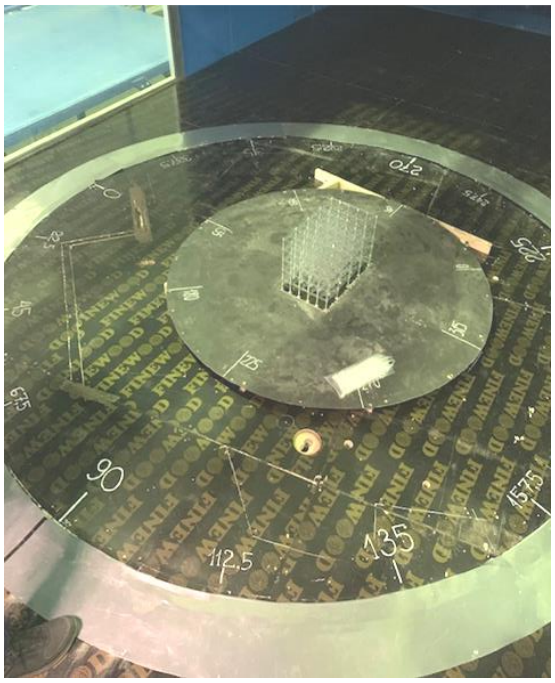


Figure 6. Scheme of the turntable with a mounted aeroelastic model.

In the beginning of the experiment, the permeable structure is mounted in the position of the angle of incidence β = 0°, and "zero" (in the absence of the air flow) readings of the load-cell type scale are taken which is required for accounting for the initial displacement value when the sensor is loaded by the aeroelastic model structure dead weight only. By rotating the turntable with the mounted aeroelastic model in the wind tunnel, the angle of incidence of the wind air flow is changed from 0° to 360° with a pitch of 45° (Figure 6).

Load-cell scale readings are recorded during the test run for each angle of incidence of the wind air flow. After that, wind protection screens are mounted onto the aeroelastic model, and the recording of the load-cell scale readings is repeated for each angle of incidence of the wind flow. For the sequence of the screen mounting options on the facade of the structure, see Figure 7.

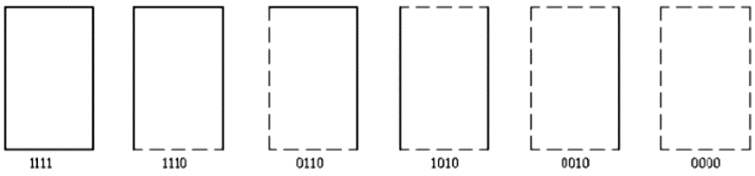


Figure 7. Arrangement of wind protection screens.

First, the wind effect test is performed with the open structure, without wind screens (Option (0000)); then, the test is consequently performed for the structure with one mounted screen on the long side (Option (0010)), with two screens on parallel sides (Option (1010)), two screens on adjoining sides (Option (0110)), three screens (Option (1110)), and with the structure closed all around (Option (1111)).

3. Experimental Results: Aeroelastic Data Analysis

3.1. Experimental Data

As a result of experimental testing, force and torque specifications are obtained for the installation area of the load cells in the base of the canceled structure when a steady air flow is applied. Thereby, the following is considered:

- a change in β wind flow angle of incidence from 0° to 360° with 45° pitch;

- facade screen mounting sequence from a completely open structure (Option (0000)) to a completely closed one (Option (1111)).

The first test is performed for a completely permeable structure (Option (0000)).Table 1 specifies forces Fx, Fy, Fz (tf), bending torques Mx, My, torque Mz (tf*m) for Option (0000).

Table 1. ForcesFx, Fy, Fz (tf), bending torques Mx, My, torque Mz (tf*m)for an open model, angle of incidence (degree), Option (0000).

Angle of Incidence, Degree	F_x (tf)	F_y (tf)	F_z (tf)	M_x (tf*m)	M_y (tf*m)	M_z (tf*m)
0	1.75	4.79	2.03	−0.29	0.00	−0.01
45	−1.88	4.25	2.65	−0.25	−0.28	0.01
90	−4.21	−0.74	0.44	0.07	−0.34	−0.01
135	−4.76	−5.04	1.62	0.37	−0.27	−0.01
180	−2.93	−5.58	0.92	0.40	0.06	−0.01
225	2.79	−4.34	0.27	0.30	0.32	0.01
270	4.42	0.32	0.12	0.00	0.35	−0.01
315	5.09	4.72	1.81	−0.28	0.26	−0.01

The second test is performed with one wind protection screen mounted on the long side of the aeroelastic model: Option (0010). The third test is performed using the aeroelastic model with two mounted wind protection screens, parallel to each other: Option (1010). The fourth test is performed using the aeroelastic model with two wind protection screens mounted on the adjoining sides: Option (0110).

The fifth test is performed using the aeroelastic model with three mounted wind protection screens: Option (1110). The sixth test is performed using the aeroelastic model with four mounted wind protection screens completely closing the structure: Option (1111). Table 2 specifies forces Fx, Fy, Fz (tf), bending torques Mx, My, torque Mz (tf*m) for the closed aeroelastic model, Option (1111).

Table 2. Forces Fx, Fy, Fz (tf), bending torques Mx, My, torque Mz (tf*m) for the closed aeroelastic model, Option (1111).

Angle of Incidence, Degree	F_x (tf)	F_y (tf)	F_z (tf)	M_x (tf*m)	M_y (tf*m)	M_z (tf*m)
0	3.61	12.85	7.78	−0.74	−0.02	0.04
45	−2.54	12.10	7.52	−0.65	−0.40	0.09
90	−6.43	−0.19	5.60	0.01	−0.46	0.06
135	−7.04	−12.74	3.90	0.67	−0.30	−0.12
180	−3.51	−13.17	3.48	0.75	−0.05	0.05
225	3.59	−11.03	3.46	0.61	0.41	0.06
270	6.38	2.64	5.55	−0.14	0.45	0.06
315	8.98	12.41	7.32	0.71	0.33	−0.07

The obtained torque values indicate that Mz torque is equal to zero due to the symmetry of the structure and the effects, as well as the location of measurement transducers in the base on the first level of the structure located on the OZ vertical symmetry axis of the structure. Mx, My bending torques for the aeroelastic model are also small, whether or not it is open or closed with wind protection screens. Fz values for the open aeroelastic model are less than Fx, Fy values.

When the screens are mounted on all four sides, the stiffness of the structure is increased, and the spatial factor influences the behavior of the structure.

If the aeroelastic model is completely closed with wind protection screens, as per Option (1111), the highest force Fz = 7.3–7.5 (tf) is observed at the incidence angles of 45°,

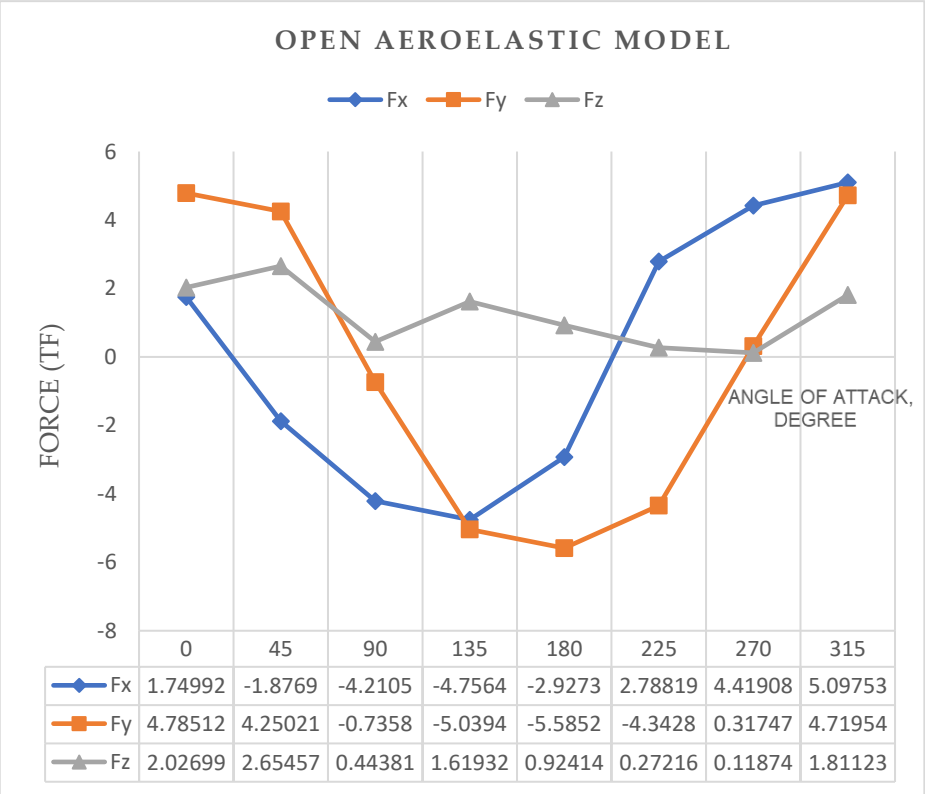
315°. For a totally permeable, open aeroelastic model, values of Fz = 2.03–2.65 (tf) are higher than other Fz values for an open aeroelastic model, and have no similar values at a symmetrical swing of the structure, which is why they contain a measurement error. Individual errors of the force values are determined by the experiment error.

3.2. Analysis of the Force and Torque Specifications of the Aeroelastic Model

The obtained forces Fx (tf), Fy (tf) are analyzed for different options of installation of protective screens and angles of attack of the wind flow.

3.2.1. Match of Force and Torque Data for Screen Mounting Options (0000) and (0010)

Figure 8 shows force curves of Fx, Fy, Fz (tf) for a change in the angle of attack from 0° to 360° for the open aeroelastic model, Option (0000). Figure 9 shows force diagrams of Fx, Fy, Fz (tf) for a model with the facade on one long side, Option (0010).



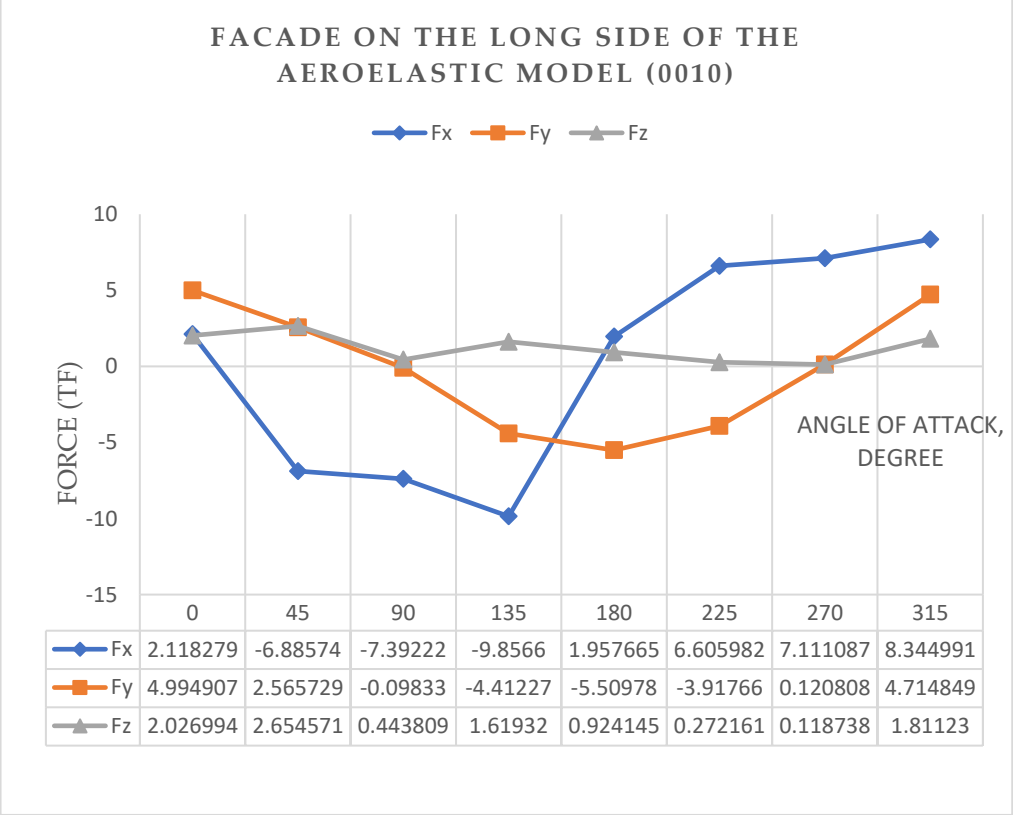
	0	45	90	135	180	225	270	315
Fx	1.74992	-1.8769	-4.2105	-4.7564	-2.9273	2.78819	4.41908	5.09753
Fy	4.78512	4.25021	-0.7358	-5.0394	-5.5852	-4.3428	0.31747	4.71954
Fz	2.02699	2.65457	0.44381	1.61932	0.92414	0.27216	0.11874	1.81123

Figure 8. Force curves of Fx, Fy, Fz (tf) for a change in the angle of attack from 0° to 360°, for an open aeroelastic model, Option (0000).

The obtained data indicate an increase in Fx values for the case with one protection screen mounted on the long side (Option (0010)) as compared with the forces for the open aeroelastic model grid (Option (0000)). So, for angles of 135°, 315° there is almost a double increase.

Thereby, the greatest values are observed at angles of 135° and 315°. For open lattice (Option (0000)), at 135°, Fx = −4.8 (tf). For an aeroelastic model lattice with one side screened (Option (0010)), maximum values at 135° make Fx = −9.9 (tf), whereas at 315°the maximum values are Fx = 8.3 (tf).

That is why, for one-sided screening of the aeroelastic model (Option (0010)), the worst case is the incidence angle of 135°, when the windward side is screened.



	0	45	90	135	180	225	270	315
Fx	2.118279	-6.88574	-7.39222	-9.8566	1.957665	6.605982	7.111087	8.344991
Fy	4.994907	2.565729	-0.09833	-4.41227	-5.50978	-3.91766	0.120808	4.714849
Fz	2.026994	2.654571	0.443809	1.61932	0.924145	0.272161	0.118738	1.81123

Figure 9. Force curves of Fx, Fy, Fz (tf) for a change in the angle of attack from 0° to 360°, for an open aeroelastic model with a facade on the long side, Option (0010).

For Fy values, as per Figures 8 and 9, there are two cases close to each other in terms of values and distribution: an open structure (0000) and a closed long side (0010). Due to the symmetry of the structure and the arrangement of sensors in the middle of the symmetry plane on the OZ symmetry axis and at a sufficient distance between the screen and the force measurement point, the influence of the screen mounting is of negligible effect for the Fy force value change as compared to the open structure case.

3.2.2. Match of Force and Torque Data for Screen Mounting Options (0000) and (1010)

Force curves of Fx, Fy, Fz (tf) for an aeroelastic model with two fronts on the long sides (Option (1010)), when the angle of attack changes from 0° to 360°, are shown in Figure 10.

For force values of Fx, as per Figures 8 and 10, there are two cases, the open structure (0000) and the symmetrically screened structure (1010), which close to each other in terms of values and similar in terms of distribution due to the symmetry of the wind screen arrangement.

The difference between Fy frontal forces for Options (0000) and (1010) is significant. The presence of symmetrical screens contributes to an increase in Fy values due to the additional dynamic pressure triggered by the mounted screens.

The greatest force values of Fy = −18.1 (tf) are observed at 180°(or 0°), whereas for other angles of 45°, 135°, 225°, and 315° greater Fy values are from 15 to 15.7 (tf), which are almost triple the Fy forces for the same angles of incidence of the wind flow in Option (0000), when the structure is open.

For the angles of incidence of 90° and 270°, a decrease in the modulus of the force values of Fy = 2.8 (tf), Fy= −3.0 (tf) is stipulated by the circumstance that long screened sides are perpendicular to the flow direction, and frontal forces become angular.

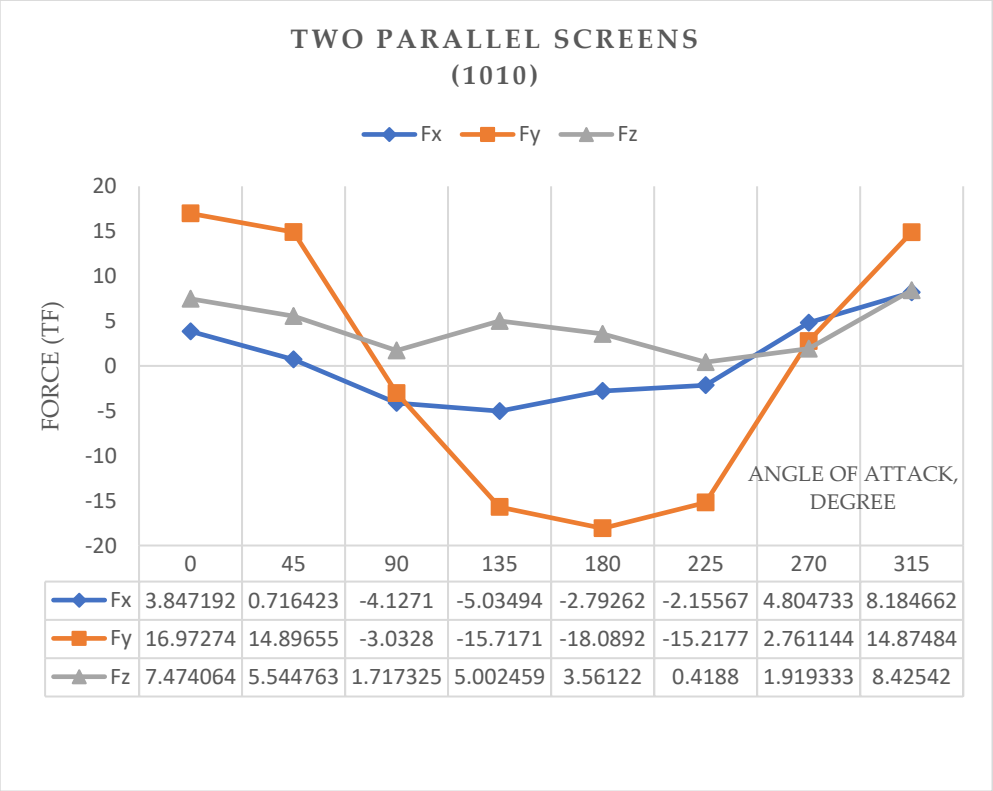


Figure 10. Force curves of Fx, Fy, Fz (tf) when the angle of attack is changed from 0° to 360° for an aeroelastic model with two parallel screens, Option (1010).

3.2.3. Matching Force and Torque Data for Screen Mounting Options (1110) and (1111)

Force curves of Fx, Fy, Fz (tf) with a change in the angle of attack from 0° to 360° for the closed model (Option (1111)) are shown in Figure 11.

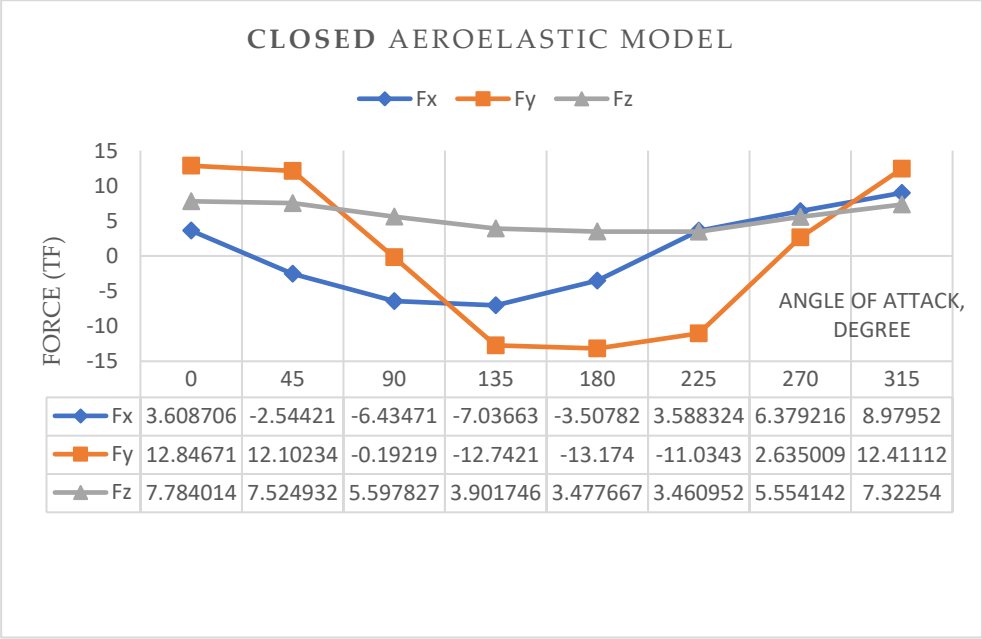


Figure 11. Force curves of Fx, Fy, Fz (tf) when the angle of attack is changed from 0° to 360° for a closed aeroelastic model, Option (1111).

For force values of Fx, Option (1111) of the aeroelastic model with all-around screening and Option (1110) of the aeroelastic model, with one short side open, are close to each other in terms of values and the force distribution, due to the symmetry of the structure. The difference in the force values of Fx is observed at the swing of the structure by 45° in the wind air flow direction.

Placing the aeroelastic model on the short windward side of the flow without screens at an angle of 45° leads to an increase in axial forces of Fx by 75%.

In general, aeroelastic model maximum values for protection screen arrangement options with three closed sides (1110) and with all closed sides (1111) are reached at the angles of incidence of 135°, 315°, corresponding to the worst case of the structure position for Fy axial forces.

3.2.4. Matching Force and Torque Data for Asymmetrical Protection Screen Arrangement Options ((0110), (0010), (1110)), in Comparison with Open (Option (0000)) and Completely Closed (Option (1111)) Aeroelastic Model Options

Asymmetrical wind protection screen arrangement greatly contributes to an increase in Fx axial forces in the aeroelastic model for wind screen arrangement Options (0110), (0010).

In general, the asymmetry of the wind protection screen arrangement is displayed to a great extent for Fx axial forces in the case of two adjoining screened sides, as per Option (0110), contributing to an increase in Fx and the greatest values of Fx, as compared to other screen arrangements.

For 315°, the greatest Fx values are observed for Option (0110), with two screened adjoining sides: Fx = 11.3 (tf). For the same angle of incidence of 315°, Fx force values for an asymmetrical wind protection screen arrangement are close to Fx= 8.3 (tf), being a little less than that of a completely closed aeroelastic model, as per Option (1111): Fx = 9.0 (tf).

For the asymmetrical wind screen arrangement (Options (0110), (1110), (1111)), as per Figure 10, the greatest forces of Fy = 14.4 (tf) are observed for the aeroelastic model in the case of Option (0110) with two adjoining screened sides at 315°(long windward side with the wind protection screen).

As compared with the open model, the asymmetrical arrangement of wind protection screens on the aeroelastic model for Options (0110) and (1110), as well as the completely closed aeroelastic model, as per Option (1111), leads to more than a double increase in the Fy force values.

The result of the data analysis demonstrates that the most complicated case for Fy force values leading to an increase in Fy values is the symmetrical arrangement of wind protection screens on the long side parallel to the approaching wind flow direction. Maximum force values of Fy = 18.1 (tf) are reached at a 180° angle of incidence of the wind air flow.

Asymmetrical arrangements of the screens for Options (0110) and (1110), as well as for Option (1111), lead to close values and similar distributions of frontal forces of Fy, greater than those of the open aeroelastic model and the aeroelastic model with the screen mounted on one side.

The greatest Fz forces occur in the case of the mounting of two parallel screens, as per Option (1010): Fz = 8.4 (tf), at an angle of incidence equal to 315°. The same Fz values are observed for the structure completely closed with wind protection screens. The least (negligible) forces occur while testing the completely open aeroelastic model structure, as per Option (0000): Fz = 2.8 (tf), at a 180° angle of incidence, as well as while testing the aeroelastic model with the wind protection screen on one side, as per Option (0010): Fz = 0.44 (tf), at an angle of incidence equal to 90°.

Based on Fx, Fy values, the resulting R force is plotted in the XOY plane [31–33]. Based on R force in XOY, and Fz component, a resulting force in the load cell mounting area is plotted. These forces are analyzed in detail in papers [31–33].

Figures 12 and 13 show values and directions of forces of Fx, Fy in the aeroelastic model in the XOY plane for the angles of wind flow attack equaling 00 and 1350, respectively, and for an open aeroelastic model (Option (0000)).

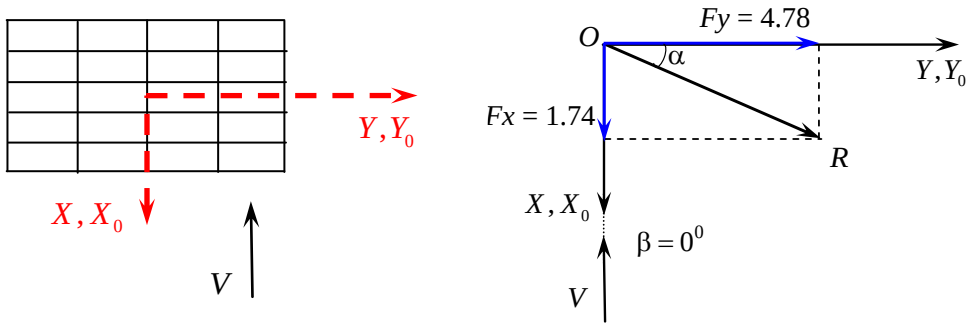


Figure 12. Direction of forces in the section at the angle of attack $\beta = 0°$.

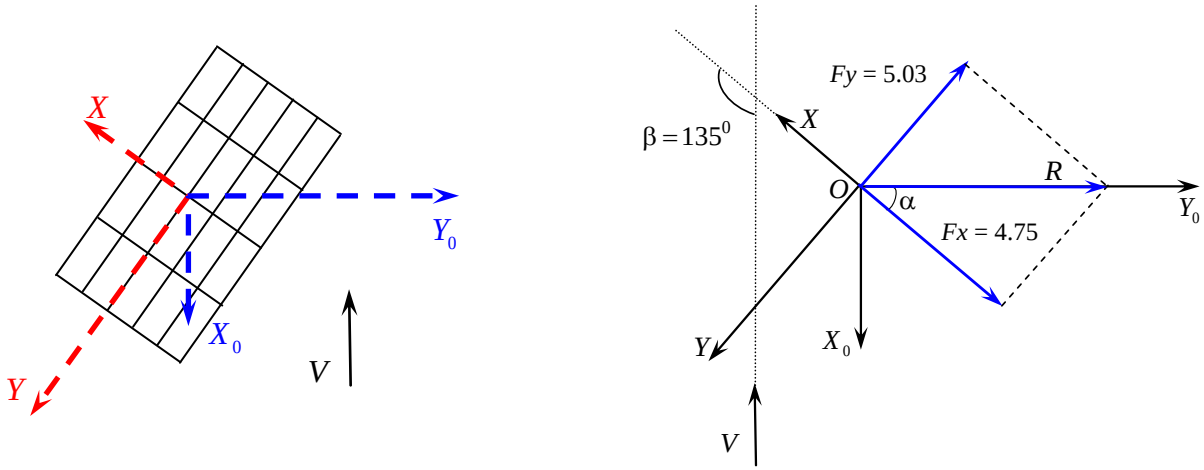


Figure 13. Direction of forces in the section at the angle of attack $\beta = 135°$.

For example, Table 3 has forces of Fx, Fy, and Fz, the equilibrium vector R of forces of Fx, Fy (tf) in the XOY plane, and the equilibrium vector Rz of the space component of forces of Fx, Fy, and Fz for the open aeroelastic model.

Table 3. Distribution of forces of Fx, Fy, and Fz (tf) and their resulting vector R (tf) in the XOY plane and in the Rz (tf) space for the open aeroelastic model, Option (0000).

Angle of Incidence, Degree	Component F_x (tf)	Component F_y (tf)	Component F_z (tf)	Resulting in Plane R (tf)	Resulting Force Rz (tf)
0°	1.749	4.785	2.026	5.08	5.4765
45°	−1.876	4.250	2.6547	4.64	5.3494
90°	−4.210	−0.735	0.4439	5.08	5.669
135°	−4.7564	−5.039	1.6193	6.92	7.1467
180°	−2.927	−5.585	0.9241	6.29	6.3578
225°	2.788	−4.342	0.2721	5.15	5.1533
270°	4.419	0.317	0.118	4.43	4.43
315°	5.097	4.719	1.8112	6.94	7.1789

4. Results

- Experimental aeroelastic studies of the steady wind effect on an aeroelastic model of a canceled structure, rectangular in the layout, were conducted under recognition of the following:
  - (1) Different angles of incidence of the wind air flow;

(2) mounting arrangement of wind protection screens.

Six arrangement options of protection screens for different angles of incidence of the approach of steady wind flow acting on the aeroelastic model were considered.

- Analysis of internal forces of the aeroelastic model in the load cell mounting area was carried out. The most unfavorable loading case is observed in the following conditions:
  1. For the completely permeable structure, the maximum resulting force of 7.1 (tf) is observed at 135° and 315° angles of incidence of the wind flow.
  2. Mounting of one wind protection screen on a long side of the aeroelastic model structure leads to a greater maximum resulting force of up to 11 (tf) at a 135° angle of incidence of the wind flow.
  3. Mounting of two parallel screens leads to a further increase in the resulting force value up to 19 (tf) at 0°, 180°, 135°, 315° angles of incidence of the wind air flow.
  4. Mounting of two screens on adjoining sides leads to occurrence of forces of 18.4 (tf) and 16 (tf) at 0° and 315° angles of incidence, respectively.
  5. Mounting of three screens slightly reduces the resulting force down to 16.8 (tf)at a 315° angle of incidence.
  6. If the aeroelastic model is closed with wind protection screens on all sides, the resulting force value is close to that for the aeroelastic model with three wind protection screens, assuming the value of 16.6 (tf) at a 315° angle of incidence of the wind flow.

It is not recommended to erect the full-scale structure with such wind protection screen arrangement options with the predominant wind direction coincident with the specified wind flow directions.

5. Discussion

The paper focuses on an experimental study of the wind effect on a canceled structure. The aeroelastic model was erected in the wind tunnel section with flat steady air flow conditions. The experimental study of the air flow effect on the structure was conducted in the flow area where the flat steady flow was reduced to a single-axis vortex-free steady flow; thereby, for the specific wind air flow velocity, self-similarity by the Reynolds number was valid. The wind flow producing the effect on the structure and the angle of incidence of the wind air flow were considered constant in terms of the exterior surface of the structure. Additionally, the steady nature of the flow passing through the structure may be considered as a test gas dynamics model allowing for the analysis of internal forces under recognition of the influence of the wind flow direction on the structure under test.

In the course of the experiment, the effect of the wind flow on the internal forces within the canceled structure was studied, with account taken of the mounting arrangement of wind protection screens. Aeroelastic model studies of unique buildings in wind tunnels also include the identification of the aerodynamic factor of external pressure distribution (Cp) across the surface of the tested object and the identification of integral aerodynamic factors of drag (Cx), transversal force (Cy), and torque (Mz). The readings of the load-cell scale allow deriving of the dynamic factor. During the design analysis and numerical modeling of the wind flow effect on the structure, the designer may need to analyze the dynamic factors based on the experimental data. Towards this end, it may be necessary to finalize the modeling conditions: the total wind load on the structure, the pulse component of the wind load, the wind pressure onto the structure surface, areas of unsteady air motion, and areas of air flow interaction with the facility.

No modeling of changes in the size of the canceled structure, rectangular in the layout, was conducted. During the experiment, the influence of the position of the canceled structure on internal forces was studied using different protection windscreen arrangement options relative to the wind effect direction. This allows selecting the structure position and the wind protection screen arrangement, with specified dimensions, that are optimal for the structure operation and comfortable work of people under the wind effect.

6. Conclusions

The experimental aerodynamic studies of the wind effect on a canceled structure, rectangular in the layout, allow for the analysis of wind effects on forces and torques occurring within the structure with account taken of the wind flow velocity directions and different arrangements of wind protection screens on the facades.

The practical relevance of the paper consists in the future recommendations on the optimum position of a canceled structure, subjected to a specific wind effect, and on the arrangement of wind protection screens to ensure the optimal operation of the structure and comfortable work of people inside.

The tests, the obtained force and torque data, and the analysis thereof are considered as a validation stage of simulation of wind effects on a canceled structure for different arrangements of facade wind screens. Further, during the numerical modeling of the stress–strain behavior of canceled structures, one can use the obtained data for the validation of a computer model, verification of the calculation schematic and the consistency of the test results, and the stress–strain behavior of the model. Upon detection of discrepancies in the obtained results, it is possible to mutually correct the numerical modeling and the aerodynamic tests of the canceled structure under recognition of the need to model parameter changes.

The modeling of wind effects on a canceled structure includes development of a model adequately reproducing the behavior of a real structure, including the physical modeling of this effect. The experimental modeling of wind effects in a wind tunnel in the initial design stage is thereby considered as a model validation stage. It allows verifying the adequacy of the computation pattern and the numerical modeling using the obtained experimental data. Data matching allows correcting the canceled structure model subjected to a wind effect.

Author Contributions: Conceptualization, L.F. and M.L.; methodology, M.L.; software, L.F. and M.L.; validation, L.F. and M.L.; formal analysis, L.F. and M.L.; investigation, L.F. and M.L.; resources, L.F. and M.L.; data curation, L.F. and M.L.; writing—original draft preparation, L.F. and M.L.; writing—review and editing, L.F.; visualization, L.F. and M.L.; supervision, L.F.; project administration, L.F.; funding acquisition, L.F. All authors have read and agreed to the published version of the manuscript.

Funding: This research received no external funding.

Institutional Review Board Statement: Not applicable.

Informed Consent Statement: Not applicable.

Data Availability Statement: All data generated or used during the study are available from the corresponding author by request.

Conflicts of Interest: The authors declare no conflict of interest.

References

1. Retter, E. *Architectural and Construction Aerodynamics*; Stroyizdat Publishers: Moscow, Russia, 1984; 294p.
2. Simiu, E.; Skanlan, R. *Wind Effect on Structures*; Maslova, B.E., Ed.; Stroyizdat Publishers: Moscow, Russia, 1984; 360p.
3. Serebrovskiy, F.L. *Aeration of Residential Area*; Stroyizdat Publishers: Moscow, Russia, 1971; 112p, No. 3.
4. Retter, E.I.; Serebrovskiy, F.L. Aerodynamic specifications of residential buildings. *AVOK J.* **2008**, *5*, 1–7.
5. Sternin, L.E. *Basics of Gas Dynamics*; Vuzovskaya Kniga: Moscow, Russia, 2016; 332p.
6. Samsonov, V.T. *Aerodynamics of Industrial Buildings: Aerodynamic Calculations in Ventilation Emissions Design*; INFRA-M: Moscow, Russia, 2019; 230p.
7. Kazakevich, M.I. *Basics of Facility Calculations for Wind Effects. Monograph*; MSUCE: Moscow, Russia, 2019; 180p.
8. Guvernyuk, S.V.; Gagarin, V.G. Computer modeling of aerodynamic effects onto enclosure elements of high-rise buildings. *AVOK J.* **2007**, *2*, 16–22.
9. Gordeyev, V.; Lantukh-Lyashchenko, A.; Pashinskiy, V.; Perelmuter, A.; Puchugin, S.F. *Loads and Effects on Buildings and Structures*; ASV Publ.: Moscow, Russia, 2011; 528p.
10. Tabunshchikov, Y.A.; Shilkin, N.V. Aerodynamics of high-rise buildings. *AVOK J.* **2004**, *8*, 1–6.
11. Raffel, M.; Willert, C.; Wereley, S.; Kompenhans, J. *Practical Image Velometry. A Practical Guide*; Springer: Cham, Switzerland, 2007; 448p.
12. Pichugin, S.; Makhin'ko, A. *Wind Load on Building Structures*; ASMI Publ.: Poltava, Ukraine, 2005; 342p.

13. Davenport, A.G. Gust loading factors. *J. Struct. Divasion* **1967**, *93*, 11–34. [CrossRef]
14. American Society of Civil Engineers. *Minimum Design Loads for Buildings and Other Structures*; ANSI/ASCE 7-11; American Society of Civil Engineers: New York, NY, USA, 2011; pp. 9–21.
15. *SP 20.13330.2011*; Load and Effects. Updated Edition of SNiP 2.01.07-85. Minregion of Russia: 27 December 2010, No. 787, Valid since 20 May 2011. MinregionRossii Publ.: Moscow, Russia, 2010. Available online: https://www.russiangost.com/p-20775-sp-20133302011.aspx (accessed on 1 February 2023).
16. Belostotskiy, A.M.; Akimov, P.A.; Afanasyeva, I.N. *Computative Aerodynamics in Problems of Civil Engineering*; ACV PH: Moscow, Russia, 2017; 720p.
17. Bowen, A.J. The prediction of mean wind speeds above simple 2D hill shape. *J. Wind. Eng. Ind. Aerodyn.* **2019**, *15*, 259–270. [CrossRef]
18. Kent, C.W.; Grimmond, C.S.B.; Gatey, D.; Barlow, J.F. Assessing methods to extrapolate the vertical wind-speed profile from surface observations in a city centre during strong winds. *J. Wind Eng. Ind. Aerodyn.* **2018**, *173*, 100–111. [CrossRef]
19. Retter, E.I.; Strizhenov, S.I. *Aerodynamics of Buildings*; Stroyizdat Publishers: Moscow, Russia, 1968; 249p.
20. Egorychev, O.O.; Churin, P.S.; Poddaeva, O.I. Experimental study of force and moments wind loads on high-rise buildings. *Ind. Civ. Constr.* **2014**, *9*, 28–30.
21. Poddaeva, O.; Fedosova, A.; Gribach, J. The study of wind effects on the bridge constructions. In *E3S Web of Conferences*; EDP Sciences: Les Ulis, France. [CrossRef]
22. Poddaeva, O.I. Physical study of architectural-construction aerodynamics for sustainable design in construction industry. *Ind. Civ. Constr.* **2013**, *9*, 35–38.
23. Poddaeva, O.I.; Dunichkin, I.V. Architectural and Construction Aerodynamics. *Vestn. MGSU* **2017**, *12*, 602–609. [CrossRef]
24. Egorychev, O.O.; Guvernyuk, S.V.; Isaev, S.A.; Poddaeva, O.I.; Kornev, N.V.; Usachov, A.E. Numerical and physical modeling of wind effects on a group of high-rise buildings. *Vestn. MGSU* **2011**, *1*, 185–191.
25. Babich, Y.M.; Rewinkel, J.-P.; Filipchyk, S.V. Experimental Determination of Wind Load Acting on the Roof Structure of the Magdeburg Stadium. *Proc. Byeloruss. Russ. Univ.* **2014**, *1*, 126–135. [CrossRef]
26. Bulgakov, S.; Tamrazyan, A.; Stepanov, A. *Risk Reduction in Construction during Natural Catastrophes and Man-Induced Emergency Situations*; MAKS Publ.: Moscow, Russia, 2004; 297p.
27. Gnyrya, A.I.; Korobkov, S.V.; Koshin, A.A.; Terekhov, V.I. Physical simulation of wind pressureon building models at various arrangement and airflow conditions. In *IV International Research Conference "Information Technologies in Science, Management, Social Sphere and Medicine" (ITSMSSM 2017)*; Published by Atlantis Press: Amsterdam, The Netherlands, 2017; Volume 72, pp. 389–392.
28. Belostotskiy, A.M.; Dubinskiy, S.I.; Afanasyeva, I.N. Numerical modeling of construction aerodynamics problems. Development of calculation methods of wind effects and full-scale project studies. *Vestn. MGSU* **2010**, *4*, 182–185.
29. Travush, V.I.; Fedorova, N.V. Survivability of structural systems of buildings with special effects. *Mag. Civ. Eng.* **2018**, *81*, 73–80. [CrossRef]
30. Verification and Validation of Models for Engineering Calculations. Available online: https://multiphysics.ru/stati/blog/verifikatciia-i-validatciia-modelei-dlia-inzhenernykh-raschetov.htm (accessed on 19 April 2022).
31. Frishter, L.; Lukin, M. Experimental study of wind effect on multilevel industrial scaffolding. *E3S WebConf.* **2020**, *157*, 06009. [CrossRef]
32. Frishter, L.; Lukin, M. Fulfilment of the Zhucowski's Theorem Conditions in Research of the Stationary Wind Exposure to the Canceled structure. In *Proceedings of FORM 2022: Construction the Formation of Living Environment; Lecture Notes in Civil Engineering*; Akimov, P., Vatin, N., Tusnin, A., Doroshenko, A., Eds.; Springer: Cham, Switzerland, 2023; Volume 282. [CrossRef]
33. Lukin, M. Study of Wind Effect on Open Industrial Tower-Type Supporting Frames with Equipment or Protective Screen, with Shapes Close to Rectangular. Bachelor's Thesis, National Research Moscow State Civil Engineering University (MGSU), Moscow, Russia.

Disclaimer/Publisher's Note: The statements, opinions and data contained in all publications are solely those of the individual author(s) and contributor(s) and not of MDPI and/or the editor(s). MDPI and/or the editor(s) disclaim responsibility for any injury to people or property resulting from any ideas, methods, instructions or products referred to in the content.